

Cable vibration control with a semiactive MR damper-numerical simulation and experimental verification

W.J. Wu^{1,2} and C.S. Cai^{2*}

¹Mustang Engineering, Houston, TX 77084, USA

²Department of Civil and Environmental Engineering, Louisiana State University, Baton Rouge, LA 70803, USA

(Received January 23, 2008, Accepted December 1, 2009)

Abstract. Excessive stay cable vibrations can cause severe problems for cable-stayed bridges. In this paper a semiactive Magnetorheological (MR) damper is investigated to reduce cable vibrations. The control-oriented cable-damper model is first established; a computer simulation for the cable-damper system is carried out; and finally a MR damper is experimentally used to reduce the cable vibration in a laboratory environment using a semiactive control algorithm. Both the simulation and experimental results show that the semiactive MR damper achieves better control results than the corresponding passive damper.

Keywords: Magnetorheological (MR) damper; cable vibration control; semiactive control.

1. Introduction

Stay cables are susceptible to external disturbances because of their inadequate intrinsic damping. Under certain combinations of light rain and moderate wind (about 10 to 15 m/s), incidences of large-amplitude vibrations (on the order of 1 to 2 m) of stay cables have been reported worldwide for cable-stayed bridges (Ciolko and Yen 1999, Main and Jones 2001). This phenomenon is known as wind-rain induced cable vibration. Excessive cable vibrations are a potential threat to public safety and the national investment in transportation infrastructures. This issue has raised great concern in the bridge community and has been a cause of deep anxiety in the public.

Other than adding crossing ties/spacers to enhance the system damping for the cable network (Langsoe and Larsen 1987) or treating the cable surface to increase the cable aerodynamic stability (Sarkar *et al.* 1999), mechanical dampers are broadly used to mitigate cable vibrations. As a passive control method, oil/viscous dampers have been extensively studied to improve the damping for stay cables, both theoretically and practically (Watson and Stafford 1988, Pacheco *et al.* 1993, Main and Jones 2002). However, passive dampers may not be able to provide enough damping for long stay cables since they are usually located close to the lower end of the cable for aesthetics and convenient installation purposes. For the passive mechanical damper to be effective, it is commonly

*Corresponding author, Associate Professor, E-mail: Cscai@lsu.edu

believed that it should be anchored a certain distance away from the cable end. The farther away the damper, the more damping it provides. A rule of thumb is that the damper should be 2% of the cable length away from the cable end to provide a 1% additional damping for the first vibration mode.

One promising way to overcome the constraints of the passive mechanical dampers is to use the TMD-MR damper (Cai *et al.* 2006, Wu and Cai 2006b). This damper integrates the traditional tuned mass device (TMD) concept and adjustable MR dampers to form a semi-active system. Another way is to use semiactive mechanical dampers, as recommended by Johnson *et al.* (2002, 2003). They developed a control-oriented mathematical model for a sagged cable with passive, semiactive, and active dampers. Their numerical simulation results show that the vibration reduction efficiency of a semiactive damper is better than the optimal passive linear damper by 10% to 50% in terms of root mean square (RMS) response if the semiactive dampers are not placed at any node of the cable. The cost of the enhanced damping performance is a larger output damper force, approximately 5-10 times larger depending on the damper locations.

With the ability to adjust the output damping force, Magnetorheological (MR) dampers are a good choice to fulfill the semiactive control strategy. A general review of semiactive control using MR dampers in civil applications was conducted by Jung *et al.* (2004). The MR dampers for cable vibration control were first installed in the Dongting Lake Bridge, China. However, the damping adjustable feature of the MR dampers was not fully utilized since the dampers were actually used as cost-effective passive dampers (Chen *et al.* 2003). Therefore, experimental investigation is necessary for the guidance of their real applications, utilizing their full benefits in the near future. This paper is aimed to carry out an experimental investigation to eliminate the gap between the simulation and the implementation. The control-oriented cable-damper model is reviewed and established, and controllers that can work with the hardware are demonstrated. Comparisons are made focusing on the cable response and output damper forces between cables with and without a semiactive damper, control performance between different control methods, and control performance for a semiactive MR damper with different maximum currents.

2. State-space equation and control strategy

The cable-damper calculation model is shown in Fig. 1. The MR damper is placed at an intermediate point x_d , dividing the cable into two segments. The notation without subscript is used to represent either cable segment. The Cartesian coordinate system is also indicated in this figure. The left support of the cable is taken as the origin for the first segment and the right support for the second segment. Thus, the governing equation for the taut cable vibration with a damper can be written as

$$f_y + \frac{H}{\cos \theta} \frac{\partial^2 v}{\partial x^2} + F_d \delta(x - x_d) + F_s \delta(x - x_s) = m \frac{\partial^2 v}{\partial t^2} + c \frac{\partial v}{\partial t} \quad (1)$$

where f_y is the distributed cable force along the y direction; H is the horizontal component of the static tension force; θ is the cable angle measured from the horizontal axis; v is the cable dynamic displacement component along the y coordinate measured from the static equilibrium position of the cable; F_d and F_s are the output damping force of the MR damper and the reaction force of the shaker, respectively; δ is the Dirac delta function; x_d and x_s are the damper and shaker locations,

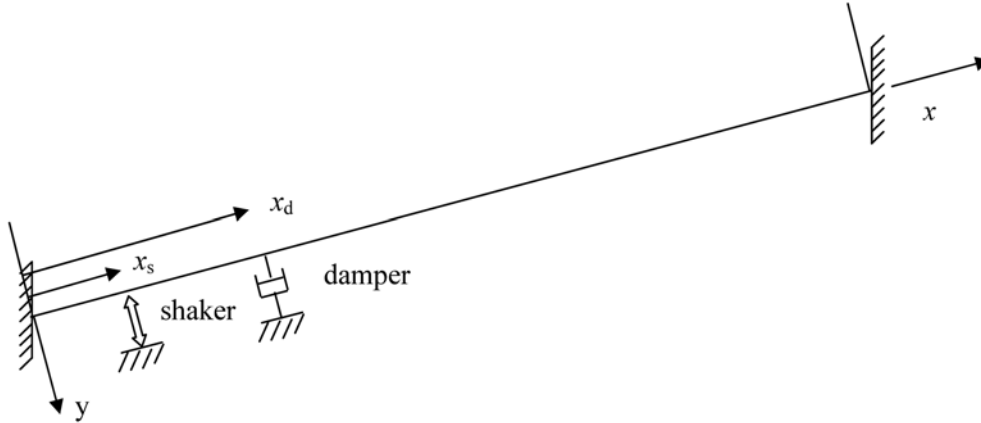


Fig. 1 Control-oriented inclined cable model

respectively; m and c are the distributed cable mass and damping coefficient per unit length, respectively; t is the time; the notation $\partial v/\partial t$ denotes the partial derivative of v with respect to “ t ” and the second partial derivatives are self-explanatory.

According to the standard Galerkin’s method, any shape function ϕ that satisfies the boundary conditions $\phi(0) = \phi(l) = 0$ can be chosen to solve the governing Eq. (1), where l is the cable length. Usually, the following sinusoid shape functions can be used

$$\phi(x) = \sin \pi j x / l \quad (2)$$

To build up an accurate and efficient control-oriented model for application, the number of shape functions is an important consideration since each shape function is actually one degree of freedom (DOF) in the generalized dynamic equation. Too many shape functions may cause the semiactive computation of the controller to become impractical. Pacheco *et al.* (1993) uses sinusoid shape functions only, needing 350 DOFs to obtain accurate results. Yu and Xu (1998) proposed a finite element based hybrid method, which also requires numerous DOFs. Johnson *et al.* (2003) suggested using the static cable profile as one of the shape functions, as well as the sinusoid shape functions. This approach largely reduced the number of required shape functions, which insured the successful semiactive control strategy with a low order, control-oriented model. Based on the simulation study by Johnson *et al.* (2003), they concluded that 21 terms, including one triangle shape function for the damper effect and 20 sinusoid functions, can provide better accuracy than several hundred sinusoid-only terms.

For the taut cable considered in the present study, the following two triangle shape functions are used to count for the effect of the damper and the shaker, respectively

$$\phi_d(x) = \begin{cases} x/x_d, & 0 \leq x \leq x_d \\ (l-x)/(l-x_d), & x_d \leq x \leq l \end{cases} \quad (3a)$$

$$\phi_s(x) = \begin{cases} x/x_s, & 0 \leq x \leq x_s \\ (l-x)/(l-x_s), & x_s \leq x \leq l \end{cases} \quad (3b)$$

Similar to Johnson’s work, 20 sinusoid functions are used. With these shape functions, the

displacement of the cable can be computed as

$$v(x, t) = \sum_{j=1}^k q_j(t) \phi_j(x) \quad k = 1 \dots 22 \quad (4)$$

Since the distributed force f_y is not considered in the current study, substituting Eq. (4) and the corresponding shape functions into Eq. (1), the generalized discrete dynamic equation for the cable-MR damper system can be written as

$$\mathbf{M}\ddot{\mathbf{q}} + \mathbf{C}\dot{\mathbf{q}} + \mathbf{K}\mathbf{q} = \mathbf{F}_s\Phi(\mathbf{x}_s) + \mathbf{F}_d\Phi(\mathbf{x}_d) \quad (5)$$

where \mathbf{q} , $\dot{\mathbf{q}}$, and $\ddot{\mathbf{q}}$ are the generalized displacement, velocity, and acceleration, respectively. The contents of the mass matrix \mathbf{M} , the damping matrix \mathbf{C} , and the stiffness matrix \mathbf{K} can be found in Johnson *et al.* (2002) for the taut cable model. The damping matrix \mathbf{C} is proportional to the mass matrix and can be determined by the distributed c value. A first modal damping of 0.5% is assumed to avoid infinite resonance response, from which $c = 0.378 \text{ N}\cdot\text{s}/\text{m}^2$ and the modal damping for other modes can be obtained. \mathbf{F}_s is the external loading simulated by the force due to the shaker, which has the feature of white noise. $\Phi(\mathbf{x}_s)$ and $\Phi(\mathbf{x}_d)$ are the load vectors for the excitation force and the damper force, respectively. Their contents are the values of the shape functions in Eqs. (2) and (3) at x_s and x_d , as

$$\Phi(\mathbf{x}_s) = [1 \quad x_s/x_d \quad \sin(\pi x_s/l) \quad \dots \quad \sin(20\pi x_s/l)]^T \quad (6a)$$

$$\Phi(\mathbf{x}_d) = [(l-x_d)/(l-x_s) \quad 1 \quad \sin(\pi x_d/l) \quad \dots \quad \sin(20\pi x_d/l)]^T \quad (6b)$$

Thus, the state space equation and the output equation for the control-oriented model can be written as

$$\dot{\mathbf{Z}} = \mathbf{A}\mathbf{Z} + \mathbf{B}\mathbf{F}_d + \mathbf{E}\mathbf{F}_s \quad (7a)$$

$$\mathbf{Y} = \mathbf{C}_y\mathbf{Z} + \mathbf{D}_y\mathbf{F}_d + \mathbf{G}_y\mathbf{F}_s + \mathbf{v} \quad (7b)$$

where $\mathbf{Z} = [\mathbf{q} \quad \dot{\mathbf{q}}]^T$ is the state variable; \mathbf{Y} is the output vector that can be measured by the accelerometers; and \mathbf{v} is the noise vector from the measurement. Other matrices can be obtained as

$$\mathbf{A} = \begin{bmatrix} \mathbf{0} & \mathbf{I} \\ -\mathbf{M}^{-1}\mathbf{K} & -\mathbf{M}^{-1}\mathbf{C} \end{bmatrix}, \quad \mathbf{B} = \begin{bmatrix} \mathbf{0} \\ \mathbf{M}^{-1}\Phi(\mathbf{x}_d) \end{bmatrix}, \quad \mathbf{E} = \begin{bmatrix} \mathbf{0} \\ \mathbf{M}^{-1}\Phi(\mathbf{x}_s) \end{bmatrix} \quad (8a)$$

$$\mathbf{C}_y = [-\Phi\mathbf{M}^{-1}\mathbf{K} \quad -\Phi\mathbf{M}^{-1}\mathbf{C}], \quad \mathbf{D}_y = [\Phi\mathbf{M}^{-1}\Phi(\mathbf{x}_d)], \quad \mathbf{G}_y = [\Phi\mathbf{M}^{-1}\Phi(\mathbf{x}_s)] \quad (8b)$$

Since only accelerations are used for the feedback loop, location matrix Φ is determined by the placement and number of the accelerometers.

For the semiactive control with a MR damper, two correlated controllers should be designed (Johnson *et al.* 2003). The primary Linear Quadratic Gaussian (LQG) controller is designed to minimize the following cost function

$$J = \lim_{T \rightarrow \infty} E \left(\frac{1}{T} \int_0^T \left(\frac{1}{2} \mathbf{q}^T \mathbf{M} \mathbf{q} + \frac{1}{2} \dot{\mathbf{q}}^T \mathbf{M} \dot{\mathbf{q}} + R(F_d^p)^2 \right) dt \right) \quad (9)$$

where the parameter R represents the variable control weight for the feedback force of the MR damper \mathbf{F}_d^p .

With a force feedback proportional to the estimated system state, $\mathbf{F}_d^p = -\mathbf{L}\hat{\mathbf{Z}}$, the primary feedback gain can be obtained as $\mathbf{L} = R^{-1}\mathbf{B}^T\mathbf{P}$, where \mathbf{P} satisfies the algebraic Riccati equation

$$\mathbf{A}^T\mathbf{P} + \mathbf{P}\mathbf{A} - \mathbf{P}\mathbf{B}R^{-1}\mathbf{B}^T\mathbf{P} + \mathbf{Q} = \mathbf{0} \quad (10)$$

$$\text{and } \mathbf{Q} = \begin{bmatrix} 0.5\mathbf{M} & \mathbf{0} \\ \mathbf{0} & 0.5\mathbf{M} \end{bmatrix}.$$

The following Kalman filter is used to estimate the system state

$$\dot{\hat{\mathbf{Z}}} = \mathbf{A}\hat{\mathbf{Z}} + \mathbf{B}\mathbf{F}_d + \mathbf{L}_{kf}(\mathbf{Y} - \hat{\mathbf{Y}}) \quad (11a)$$

$$\hat{\mathbf{Y}} = \mathbf{C}_y\hat{\mathbf{Z}} + \mathbf{D}_y\mathbf{F}_d \quad (11b)$$

where $\mathbf{L}_{kf} = (\mathbf{P}_{kf}\mathbf{C}_y^T + \mathbf{E}\mathbf{Q}_{kf}\mathbf{G}_y^T)(\mathbf{R}_{kf} + \mathbf{G}_y\mathbf{Q}_{kf}\mathbf{G}_y^T)^{-1}$ is the estimator gain. Similarly, the matrix \mathbf{P}_{kf} satisfies the algebraic Riccati equation

$$\mathbf{A}\mathbf{P}_{kf} + \mathbf{P}_{kf}\mathbf{A}^T - (\mathbf{P}_{kf}\mathbf{C}_y^T + \mathbf{E}\mathbf{Q}_{kf}\mathbf{G}_y^T)(\mathbf{R}_{kf} + \mathbf{G}_y\mathbf{Q}_{kf}\mathbf{G}_y^T)^{-1}(\mathbf{C}_y\mathbf{P}_{kf} + \mathbf{G}_y\mathbf{Q}_{kf}\mathbf{E}^T) + \mathbf{E}\mathbf{Q}_{kf}\mathbf{E}^T = \mathbf{0} \quad (12)$$

where \mathbf{Q}_{kf} and \mathbf{R}_{kf} are the auto excitation and noise spectral density, respectively. The expectations for the excitation and the noise are required to be zero to apply the algorithm.

The semiactive MR damper used in this control-oriented strategy and simulation can be expressed by the following Bingham model (Stanway *et al.* 1985)

$$F_d = C_d\dot{v}_d + F_{dy}\text{sign}(\dot{v}_d) \quad (13)$$

where C_d is the damping coefficient, \dot{v}_d is the damper velocity, F_{dy} is the friction force, which is related to the applied current in the MR damper, and $\text{sign}(\dot{v}_d)$ means the sign of the corresponding quantity “ \dot{v}_d ”. All these parameters can be obtained from the experimental data in Wu and Cai (2006a). Fig. 2 shows the experimental data and the output force calculated by Eq. (13), corresponding to a MR current of 0.4A. Only one cycle of data is plotted in the two bottom figures for clarity.

Since the MR damper can only generate dissipative force, the output damping force must be of a different sign than the damper velocity. Therefore, the secondary controller for this particular feature can be represented by the following equation

$$I = I_{\max}H(-F_d^p\dot{v}_d) \quad (14)$$

where I is the command current sent to the MR damper; I_{\max} is the maximum current that can be applied to the damper; and H is the Heaviside function, or unit step function. In this experiment the damper velocity \dot{v}_d is obtained by integrating the corresponding measured acceleration.

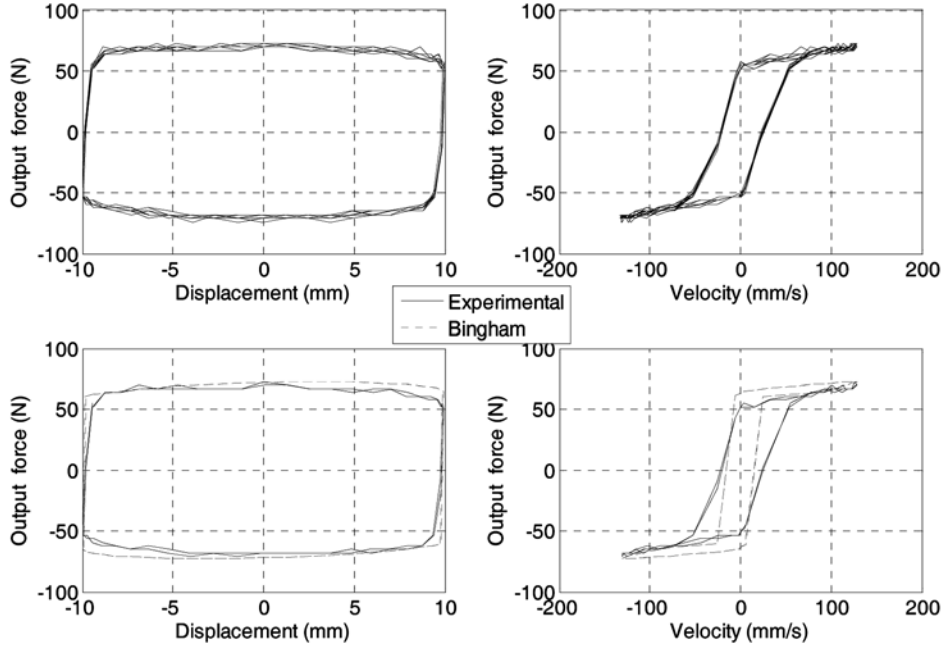


Fig. 2 Bingham model and experimental data

3. Simulation results

Before the experimental verification using a physical model can take place, a numerical simulation is carried out in the Simulink/Matlab environment to determine suitable parameters for the controller. Extensive simulation was carried out by Johnson *et al.* (2003). The present simulation done here focuses on the cable control problem at hand. The selected controller should provide a satisfactory control effect and ensure the feedback force is within the range of the capacity of the MR damper used. A block diagram for the controlled system is plotted in Fig. 3, which explains the concept described in the previous section.

Table 1 gives a comparison between the control efficiency of different control strategies, including active control, optimal passive control, MR passive control, and MR semiactive control. Two different MR properties (semiactive 1 and semiactive 2) are assumed for demonstration purposes. The active control is based on the LQG strategy shown in Eqs. (9)-(12). For optimal passive control, the optimal viscous damping is used according to Pacheco *et al.* (1993); while for MR passive control, the MR damper is turned off, i.e., with a zero current. Lastly, for MR semiactive control, the MR damper is controlled with the LQG primary and secondary control algorithms found in Eqs. (9)-(14).

The σ_{disp} is a quantity representing a mean displacement integrated along the cable, as defined by the following equation (Johnson *et al.* 2003)

$$\sigma_{disp}^2 = E \left[\int_0^l v^2(x, t) dx \right] = E \left[\frac{\mathbf{q}^T(t) \mathbf{M} \mathbf{q}(t)}{m} \right] \approx \frac{1}{m T_{exp}} \int_0^{T_{exp}} \hat{\mathbf{q}}^T \mathbf{M} \hat{\mathbf{q}} dt \quad (15)$$

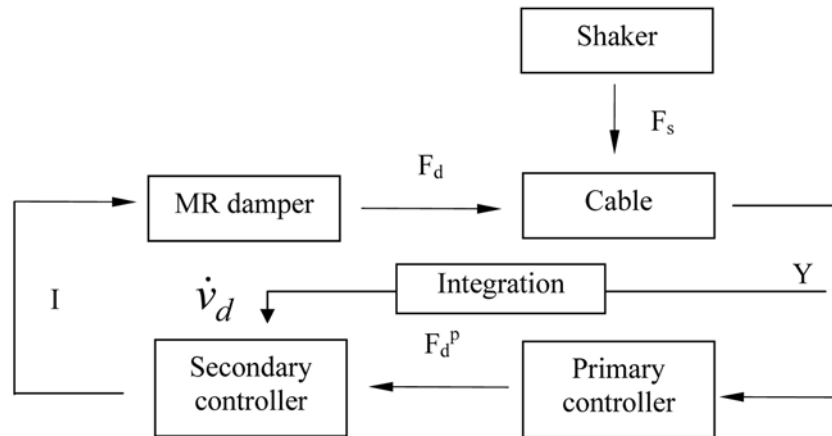


Fig. 3 Block diagram for the controlled system

Table 1 Cable vibration control with different methods (numerical simulation)

	σ_{disp} (mm)	F_d^{rms} (N)	F_d^{max} (N)
Active	1.7	9.24	24.33
Optimal passive	2.6	8.35	20.82
MR passive mode	2.2	8.55	20.80
MR semiactive 1 ($C_d = 100$ N·s/m, $F_{dy} = 40$ N)	2.0	43.78	80.38
MR semiactive 2 ($C_d = 50$ N·s/m, $F_{dy} = 10$ N)	1.7	11.91	20.84

The last approximation in Eq. (15) stems from the fact that the expected value of an ergodic quantity is equal to its time average. The state $\hat{\mathbf{q}}$ can be estimated from a similar Kalman filter with Eq. (11a). However, the output equation should change to the following equation

$$\hat{\mathbf{q}} = [\mathbf{I} \ 0] \hat{\mathbf{Z}} \quad (16)$$

From Table 1 it can be seen that the MR semiactive 1 control method can provide another 23.1% off of the integrated displacement, compared to that of the optimal passive dampers (2.0 vs. 2.6 mm). The MR semiactive 2 method reduces the displacement to 1.7 mm, which is the same as that of active control. This indicates that semiactive control may achieve similar control efficiency to the active control method if the MR damper properties are chosen properly. Even the MR passive mode can provide a better control effect than the optimal passive dampers. This comes from the fact that the MR passive mode has both the viscous and the friction force terms, which may help provide a better control effect than the optimal passive damper where only the viscous term is considered. The predicted damper output force F_d^{rms} for the MR semiactive 1 is much larger than that of the active control method, which implies that this damper output force is too large for the present cable vibration. In contrast, the MR semiactive 2 with a smaller output force, which is comparable to that of the active control, achieves a similar control effect to that of the active

control. Therefore, several smaller I_{\max} values than that used in the MR semiactive 1 are chosen in the following experimental verification.

4. Experimental setup

Scaling principles call for maintaining the similitude between the prototype cable and the model cable. However, it is actually very difficult to satisfy all the scaling principles for all the parameters in most cases. Since there is a wide range of actual cable parameters, it is only necessary to verify that the corresponding prototype stay cable is not abnormally different from the “average” value. Therefore, considering the limitations of the laboratory facility, the scaling factor n between the prototype and the model is determined as 8 according to the scaling relationship discussed by Wu and Cai (2006a).

Fig. 1 shows the setup of the cable model; the related information can be found in Table 2. Each end of the cable is anchored to a frame so that the boundary conditions are considered to be fixed ends. An adjustable tension force is applied to the cable by a hydraulic jack (Fig. 4), which can be measured accurately by a load cell (Fig. 5) with a capacity of 44480N (10 kips). The tension force is acquired by the DastarNet data acquisition system from Gould Inc. Thus, a range of the geometry-elasticity λ^2 values can be achieved by varying the tension force (see Wu and Cai 2006a for the λ^2 definition). However, in the current study, a constant tension force of 9438.7 N is used, which corresponds to a λ^2 value of 0.059. This value is in the range of 0.008-1.08, a range that covers 90% of real cables used in cable-stayed bridges based on the database collected by Tabatabai *et al.* (1998).

Table 2 Model cable parameters

Cable length (l)	7.16 m	Cable angle (θ)	11.27°
Cable cross-section area (A)	98.7 mm ²	λ^2 value	0.059
x_d	2.01 m	x_s	0.79 m

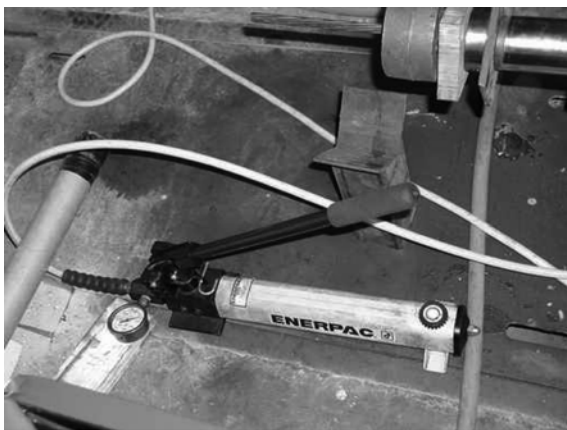


Fig. 4 Hydraulic jack

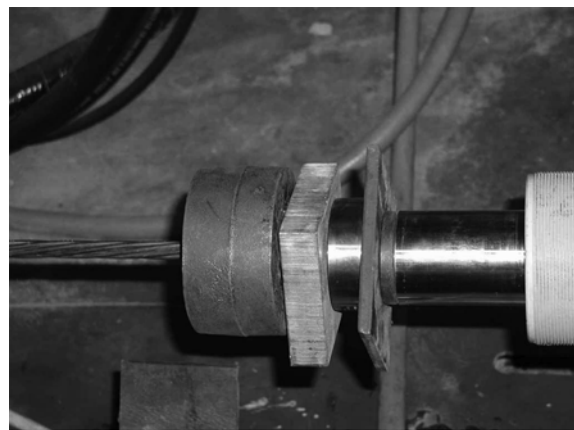


Fig. 5 10 kips load cell



Fig. 6 LDS shaker



Fig. 7 MR damper

The V408CE shaker (Fig. 6) from Ling Dynamic System Inc. located at $x_s = 0.79$ m (11% of the cable length) is used to generate the excitation for the cable vibration. The maximum output force from the shaker for a sine-wave excitation is 98N. A frame is built to facilitate the installation of the shaker perpendicular to the cable. Different forms of the excitation force can be applied by the shaker, with the magnitude measured by a load cell between the cable and the shaker. As required by the control strategy, a bandlimited white noise excitation generated from the Simulink software is used and sent to the shaker in the experiment. Before the signal goes into the shaker, a fourth order filter is used to shape the spectral content of the input energy to excite the first vibration mode of the cable. The transfer function of the filter can be expressed as (Christenson *et al.* 2006)

$$H_{sf} = \frac{\omega_f^4}{(s^2 + 0.3\omega_f s + \omega_f^2)^2} \quad (17)$$

The MR damper type RD-1097-01 (Fig. 7) purchased from Lord Cooperation is used as the semiactive damper, which can provide a maximum force level of ± 80 N at a maximum current of 0.5 ampere (Wu and Cai 2006a). The damper is located at $x_d = 2.01$ m (28% of the cable length). It is noted that the damper position here does not represent most actual applications. Similarly, a frame is provided to make the MR damper perpendicular to the cable chord and to investigate the performance of the MR damper at different locations if necessary. A load cell is placed between the damper and the cable to measure the actual force that the MR damper provides.

Two miniature accelerometers (Fig. 8) from PCB Piezotronics Inc. are used to measure the cable vibration response at different places. These accelerometers can measure up to ± 4900 m/s² acceleration with a resolution of 0.02 m/s² RMS value. These accelerometers are also used to provide input information for the Kalman filter to estimate the full state in the primary controller. One of them is at the mid-span (3.58 m) and the other is used to measure the damper acceleration, which also provides the damper velocity for the secondary controller after a numerical integration. Low pass filters with a cut off frequency of 30 Hz are used to reduce the noise before the accelerations are used.

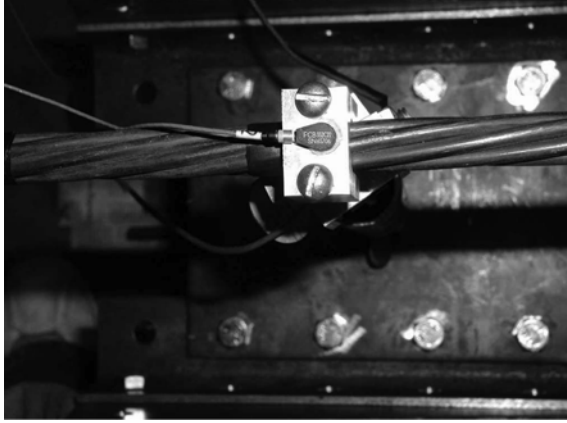


Fig. 8 PCB accelerometer

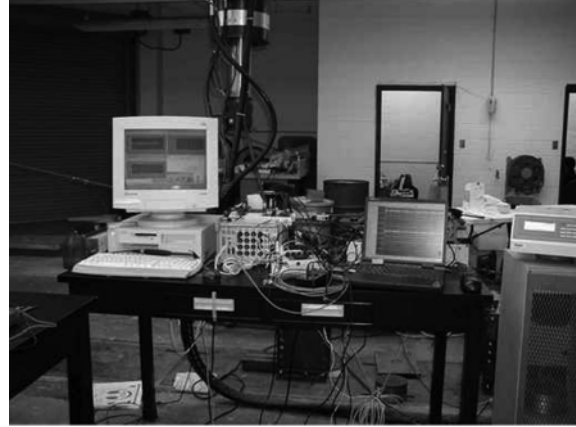


Fig. 9 Acquisition system

These two accelerations used for the controllers are acquired by a MultiQ-PCI board from Quanser Inc. This board has four available AD converters and 16 DA converters, which can accept a maximum voltage of $\pm 10\text{V}$ input and output signals. With the Wincon realtime control software built in the Simulink/Matlab environment, this board can fulfill a real time control task seamlessly. Actually, it works as an interface between the control algorithms simulated in the Matlab environment and the controlled structure. All of the signals (two accelerations, the forces from the shaker and the damper) are acquired for post processing to compare the cable response and the output damping force between the cable with and without the semiactive damper.

5. Experiment results

The experiment is carried out to verify the control strategies explained previously. As stated in Eqs. (11a), (15), and (16), the main criteria for the comparison, the integrated displacement along the cable, can be obtained by the Kalman estimator from the two measured accelerations.

Five experiments are carried out to demonstrate the effectiveness of the semiactive control, as indicated in Table 3. Before the MR damper is added to the cable, the cable vibration is measured under an excitation force of 13.09N RMS. The integrated displacement along the cable is 2.65 mm. When the MR damper is installed but is not applied with current (i.e., in the passive mode), the integrated displacement is reduced to 1.29 mm, 51% less than the uncontrolled displacement. This indicates that even if the MR damper is in its passive mode, it can still provide a considerable

Table 3 Damper control performance (experimental measurement)

	σ_{disp} (mm)	F_d^{rms} (N)	F_d^{max} (N)	F_s^{rms} (N)
Uncontrolled	2.65	N/A	N/A	13.09
MR passive mode	1.29 (51%)	4.96	13.19	15.39
Semi 0.1A	0.22 (92%)	6.54	20.45	17.15
Semi 0.2A	0.082	7.57	26.77	17.27
Semi 0.3A	0.090	7.99	34.44	17.53

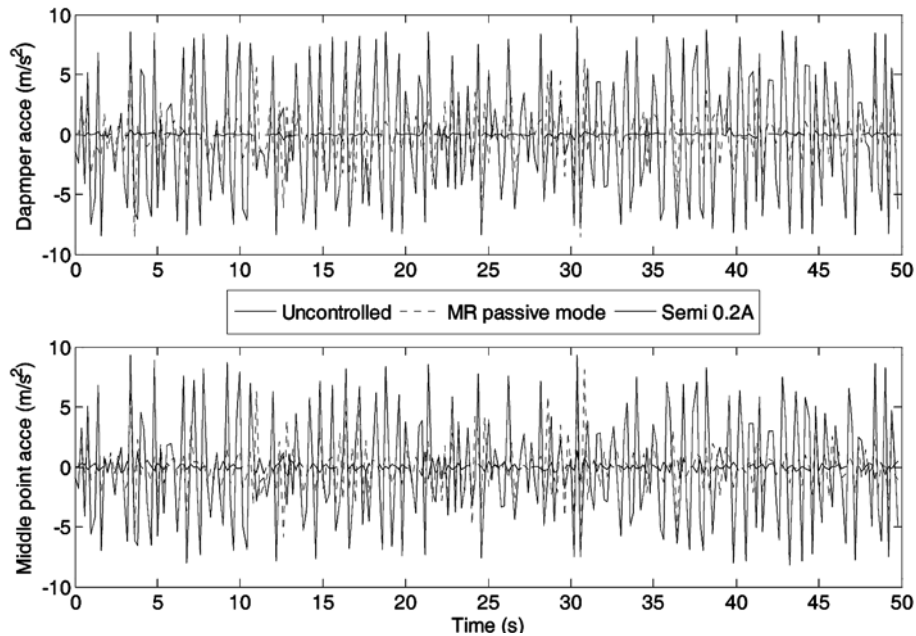


Fig. 10 Time history records for both sensors with different control strategies

reduction performance for the cable vibration. Therefore, a MR damper can work as a fail-safe device for the control strategy. The output damping force for the MR damper in passive mode is very low.

When the MR damper is working as a semiactive device, generally it can provide a better control performance. When the applied current I_{\max} is set as 0.1A, the integrated displacement is further reduced to 0.22 mm, 92% less than the uncontrolled displacement. Further increasing the current may result in a better performance, but enhanced performance is not guaranteed. As the current is increased from 0.1A to 0.2A, better damper performance is achieved by reducing the displacement from 0.22 mm to 0.082 mm. However, the performance becomes worse when the current changes from 0.2A to 0.3A. It is noted that the F_d^{\max} for the semiactive MR damper with 0.2A current is 26.77N, which is close to the simulation prediction of 24.33N for the active control shown in Table 1. This observation suggests that the MR damper may achieve the best control when its output capacity is set around its active control counterpart. Increasing the output capacity may not be beneficial to the control effect since the MR damper force may be too large for a certain level of excitation; the damper may “lock” or “freeze”.

The time history records for the measured accelerations at the damper location and the cable middle point are plotted in Fig. 10. Apparently, the semiactive MR damper gives a much better performance than the passive control, reducing the cable vibration at both sensor locations.

6. Conclusions

The current study mainly discusses the experimental verification of a semiactive control approach to reduce cable vibration. The control-oriented state-space equation and the LQG control strategy

are established. Numerical simulation results are obtained to design proper controller parameters and ensure that the demanded damper force matches the real MR damper. Experimental verification is carried out to demonstrate the concept of the MR semiactive control. Based on the simulation and experimental results, the following conclusions can be made:

1. From the simulation results, the semiactive control can achieve a better control effect than its optimal passive counterpart and a similar control effect to its active control counterpart for the cable vibration reduction. Better performance is achieved at the cost of larger control forces.
2. From the results of the experiment, even when the MR damper is in the passive mode, it still can provide a considerable control effect. Therefore, a semiactive MR damper can be a fail-safe device when the control device is not working properly in the field.
3. Also, from the experimental results, the output damping force of the semiactive damper should be set around the demand of active control at given excitation levels. Otherwise, the damper output damping force may be too large for the cable vibration, which may cause a worse control effect.

Future work may consider a refined control strategy for the secondary controller, which should provide different output current according to the severity of the cable vibration. The cable in laboratory scale is different from the in-situ cable. Therefore, how to use the experimental result to the real cable-stayed bridge is still a problem, and the gap between the simulation and the implementation still exists.

References

- Cai, C.S., Wu, W.J. and Shi, X.M. (2006), "Cable vibration reduction with a hung-on TMD system. Part I: Theoretical study", *J. Vib. Control*, **12**(7), 801-814.
- Chen, Z.Q., Wang, X.Y., Ko, J.M., Ni, Y.Q., Spencer, B.F. Jr. and Yang, G.Q. (2003), "MR damping system on Dongting Lake cable-stayed bridge", *Proceedings of Smart Systems and Nondestructive Evaluation for Civil Infrastructures*, San Diego, March.
- Christenson, R.E., Spencer, B.F. Jr. and Johnson, E.A. (2006), "Experimental verification of smart cable damping", *J. Eng. Mech.*, **132**(3), 268-278.
- Ciolko, A.T. and Yen, W.P. (1999), "An immediate payoff from FHWA's NDE Initiative", *Public Roads*, **62**(6), 10-17.
- Johnson, E.A., Baker, G.A., Spencer, B.F. Jr. and Fujino, Y. (2007), "Semiactive damping of stay cables", *J. Eng. Mech.*, **133**(1), 1-11.
- Johnson, E.A., Christenson, R.E. and Spencer, B.F. Jr. (2003), "Semiactive damping of cables with sag", *Computer-Aid. Civil Infrastr. Eng.*, **18**(2), 132-146.
- Jung, H.J., Spencer, B.F. Jr., Ni, Y.Q. and Lee, I.W. (2004), "State-of-the-art of semiactive control systems using MR fluid dampers in civil engineering applications", *Struct. Eng. Mech.*, **17**(3), 493-526.
- Langsoe, H.E. and Larsen, O.D. (1987), "Generating mechanisms for cable-stay oscillations at the FARO bridges", *Proceeding of the International Conference on Cable-stayed Bridges*, Bangkok, November.
- Main, J.A. and Jones, N.P. (2001), "Evaluation of viscous dampers for Stay-cable vibration mitigation", *J. Bridge Eng.*, **6**(6), 385-397.
- Main, J.A. and Jones, N.P. (2002), "Free vibration of taut cable with attached damper. I: Linear viscous damper", *J. Eng. Mech.*, **128**(10), 1062-1071.
- Pacheco, B.M., Fujino, Y. and Sulekh, A. (1993), "Estimation curve for modal damping in stay cables with viscous damper", *J. Struct. Eng.*, **119**(6), 1961-1979.
- Sarkar, P.P., Mehta, K.C., Zhao, Z.S. and Gardner, T. (1999), "Aerodynamic approach to control vibrations in stay-cables", Report to Texas Department of Transportation, TX.

- Stanway, R., Sproston, J.L. and Stevens, N.G. (1985), "Nonlinear identification of an electrorheological vibration damper", *IFAC Identification and System Parameter Estimation*, 195-200.
- Tabatabai, H., Mehrabi, A.B., Morgan, B.J. and Lotfi, H.R. (1998), "Non-destructive bridge technology: bridge stay cable condition assessment", Final report submitted to the Federal Highway Administration, Construction Technology Laboratories, Inc., Skokie, IL.
- Watson, S.C. and Stafford, D.G. (1988), "Cables in Trouble", *Civil Eng.*, **58**(4), 38-41.
- Wu, W.J. and Cai, C.S. (2006a), "Experimental study on magnetorheological dampers and application to cable vibration control", *J. Vib. Control*, **12**(1), 67-82.
- Wu, W.J. and Cai, C.S. (2006b), "Cable vibration reduction with a hung-on TMD system, Part II: Parametric study", *J. Vib. Control*, **12**(8), 881-899.
- Yu, Z. and Xu, Y.L. (1998), "Mitigation of three dimensional vibration of inclined sag cable using discrete oil dampers-I. formulation", *J. Sound Vib.*, **214**(4), 659-673.